

Model updation using multiple parameters influencing servoeelastic response of a flexible aircraft

Prabha Srinivasan^{*1} and Ashok Joshi^{2a}

¹Aeronautical Development Agency, PB 1718, Vimanapura Post, Bengaluru 560017, India

²Department of Aerospace Engineering, Indian Institute of Technology, Powai, Mumbai 400076, India

(Received September 10, 2015, Revised June 30, 2016, Accepted July 1, 2016)

Abstract. In a flexible airvehicle, an assessment of the structural coupling levels through analysis and experiments provides structural data for the design of notch filters which are generally utilized in the flight control system to attenuate the flexible response pickup. This is necessitated as during flight, closed loop control actuation driven with flexible response inputs could lead to stability and performance related problems. In the present work, critical parameters influencing servoeelastic response have been identified. A sensitivity study has been carried out to assess the extent of influence of each parameter. A multi-parameter tuning approach has been implemented to achieve an enhanced analytical model for improved predictions of aircraft servoeelastic response. To illustrate the model updation approach, initial and improved test analysis correlation of lateral servoeelastic responses for a generic flexible airvehicle are presented.

Keywords: servoeelastic response; lateral dynamics; sensitivity study; multi-parameter updation

1. Introduction

In the present study, a linear mathematical model is used to assess servo-elastic (SE) responses for a generic flexible aircraft. The longitudinal, lateral and directional responses are estimated in the form of transfer functions of sensor response to input control surface excitation. These vehicle responses arising from structure-control coupling comprise of both rigid and elastic components. The elastic response needs to be attenuated, as it could drive the actuator commands which would be detrimental to stability, performance and handling qualities of the aircraft.

The need for estimation of structure control coupling interactions is well established today, based on earlier flight experiences. Some instances of structure control coupling that have occurred are reported in the literature. One of the earlier occurrences is the B-36 autopilot developed in 1948, where sensor pickup of fuselage bending was experienced and solved by shifting the sensor package (Felt *et al.* 1979). In the YF-16, ASE instability was experienced at high subsonic Mach number and was attributed to coupling between the flight control system and the antisymmetric pitch mode of wing tip missile (Felt *et al.* 1979, Allen *et al.* 1986). It was corrected by appropriate notch filter design. Other instances of aeroservoelastic instabilities

*Corresponding author, Scientist, E-mail: prabha@jetmail.ada.gov.in

^aProfessor and Head, E-mail: ashokj@iitb.ac.in

described in Felt *et al.* (1979) are related to the YF-17, F-4 and the B-52 CCV. In the YF-17, FCS modifications were made to minimize ASE interactions. Pitch-roll coupling aided by flap resonance in the F-4 was solved by pitch path filtering. In the B-52 CCV RCS (Arnold and Murphy 1976), SE instability was found to be due to local support vibrations, and was solved by changing the accelerometer mounting. In Peloubet (2006), the effects of aeroservoelastic interactions in two high performance fighters with fly-by-wire control are brought out. The first aircraft showed antisymmetric oscillations in early flight tests, which was corrected by adjusting control loop gain. The second aircraft, a fighter prototype showed a pitching motion in a narrow range of high-subsonic Mach numbers, at a frequency between the first symmetric vibration mode of the structure and the rigid-body short-period mode. The problem was rectified by reducing the pitch loop gain. Buffet induced structure control coupling was experienced in the X-29A aircraft (Voraceck and Clarke 1991). Another instance is given in Wray (1999), for F-22 aircraft, at certain flight conditions corresponding to a specific speed, altitude and AOA, higher response was recorded at feed-back sensors which could be attributed to impact of separated flow and buffeting. A summary of the structural coupling approach on the F-22 aircraft is also given in Wray (1999). It is brought out that introduction of the spin recovery chute system on the rear fuselage caused a considerably lower fuselage bending frequency, which necessitated a notch filter redesign. A structural filter was also designed for the pitch stick path based on a reported PIO. Aeroservoelastic interactions and the current procedures related to design, verification and clearance are described in Becker *et al.* (2000), Luber (2009).

Enhancement of modeling and analysis procedures to accurately predict aeroservoelastic interactions and experimental validation of theoretical developments is emphasized in (Noll 1990). The need for robust analytical response predictions is also brought out in Mottershead and Friswell (1993), Vaccaro *et al.* (1995). Aircraft dynamic tests should also be carried out with diligence as they form the basis for certification and provide data for validation of analytical assessments. Instrumentation, sensor placement, input excitation and data processing in respect of full scale aircraft ground vibration tests (GVT) have been explored in Lai and Yang (1995), Peeters *et al.* (2008), Pickerel *et al.* (2006).

In the present study, analytical predictions of servo-elastic responses of a generic flexible aircraft were computed and validated with experimental results generated through conduct of Ground Vibration tests (GVT) and Structural Coupling tests (SCT). While aircraft natural frequencies are a function of mass and stiffness, the factors influencing gain amplitude of lateral servo-elastic response are identified. Parameter identification and model updation approach for longitudinal responses was studied earlier (Joshi *et al.* 2014). The focus of the present work is on the lateral response of an aircraft and modes of interest are wing antisymmetric bending (WAB), fuselage roll (FR) and fuselage lateral bending (FLB). Expressions for the peak modal responses associated with roll rate and lateral acceleration are derived. A sensitivity study is carried out by a limited perturbation of identified parameters influencing servoelastic response. By a systematic tuning of these parameters, the analytical model is updated to arrive at a better test-analysis correlation of lateral servoelastic response.

2. Mathematical formulation

Servoelastic responses for a generic flexible airvehicle were computed at the sensor locations for a unit harmonic command to control surface actuators. Longitudinal, lateral and directional

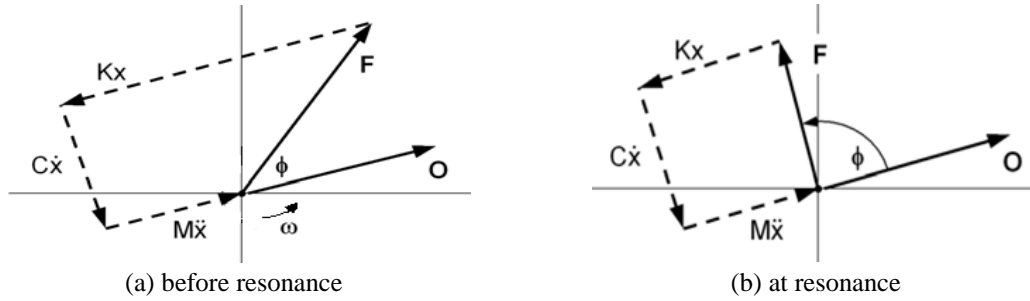


Fig. 1 Set of forces acting on a system

responses were assessed for symmetric, antisymmetric wing control surface excitation and for rudder excitation respectively. To illustrate, lateral acceleration response (n_y) at the fuselage mounted accelerometer is computed as

$$n_y = \ddot{T}_y + l_x \ddot{R}_z - l_z \ddot{R}_x + \sum_{ne} \xi_i \ddot{e}_i \tag{1}$$

And roll rate response (p) is given by

$$p = \dot{R}_x + \sum_{ne} \zeta_i \dot{e}_i \tag{2}$$

T_y , R_x and R_z are rigid body translation and rotations about global Y , X and Z axis, l_x and l_z are components of the sensor distance from aircraft C.G. The single and double dot superscripts refer to first and second derivatives with respect to time. The terms under the summation sign in Eqs. (1) and (2) are indicative of the elastic components. ξ_i and ζ_i are modal displacement and slope at the sensor location for the e_i^{th} flexible mode. ne is number of elastic modes considered. A convergence study was carried out and servoelastic computations were made using first sixty modes. The required displacements are computed from the basic servo-elastic equation of equilibrium

$$\begin{bmatrix} M_{qq} & M_{q\delta} \\ M_{\delta q} & M_{\delta\delta} \end{bmatrix} \begin{Bmatrix} \ddot{q} \\ \ddot{\delta}_c \end{Bmatrix} + \begin{bmatrix} 0 & 0 \\ 0 & C_{AB} \end{bmatrix} \begin{Bmatrix} \dot{q} \\ \dot{\delta}_c \end{Bmatrix} + \begin{bmatrix} (1+ig)K_{qq} & K_{q\delta} \\ K_{\delta q} & (1+ig_d)K_{\delta\delta} \end{bmatrix} \begin{Bmatrix} q \\ \delta_c \end{Bmatrix} = d \begin{Bmatrix} 0 \\ \delta_{ci} \end{Bmatrix} \tag{3}$$

where, ram response to voltage command for the actuator is represented by a no load fourth order transfer function

$$\frac{d}{s^4 + s^3a + s^2b + sc + d} \tag{4}$$

Actuator coefficients (a,b,c,d) are provided by the actuator OEM. In Eq. (3), M_{qq} and K_{qq} are the modal mass and stiffness matrices. g and g_d are the damping for elastic and control surface modes, C_{AB} is the actuator damping. q is the vector of rigid and elastic modes, δ_c refers to the control surface and actuator degrees of freedom. δ_{ci} is the harmonic command input. The aircraft rigid body and elastic modes are inertially and elastically uncoupled. The $M_{\delta\delta}$ terms are computed as the control surface moment of inertia about the hinge line. The $K_{\delta\delta}$ terms are obtained as the product of the actuator stiffness and the square of the hinge arm.

The expressions for the inertia coupling terms ($M_{q\delta}$, $M_{\delta q}$ matrices) and stiffness coupling terms ($K_{q\delta}$, $K_{\delta q}$ matrices) are computed starting from the basic Lagrange's equations

$$\frac{d}{dt} \frac{\partial T}{\partial \dot{x}_i} - \frac{\partial T}{\partial x_i} + \frac{\partial V}{\partial x_i} = Q \quad (5)$$

where, Q =Generalised force, Kinetic energy $T = \frac{1}{2}m\dot{x}^2$, Potential energy $V = \frac{1}{2}kx^2$

Expressing displacement x in terms of modal vectors (Φ and Φ_c) and generalised coordinates (q and δ_c) for the aircraft response and actuator and control surface response respectively

$$x = \phi q + \phi_c \delta_c$$

And substituting above in Eq. (5) gives expressions for inertia and stiffness coupling terms

$$\begin{bmatrix} \phi^T M \phi & \phi^T M \phi_c \\ \phi_c^T M \phi & \phi_c^T M \phi_c \end{bmatrix} \begin{Bmatrix} \ddot{q} \\ \ddot{\delta}_c \end{Bmatrix} + \begin{bmatrix} \phi^T K \phi & \phi^T K \phi_c \\ \phi_c^T K \phi & \phi_c^T K \phi_c \end{bmatrix} \begin{Bmatrix} q \\ \delta_c \end{Bmatrix} = Q \quad (6)$$

As seen from Eq. (6), inertia and stiffness coupling terms depend on control surface inertia, stiffness and the separation between control surface centre of mass and hinge line (input excitation is a unit radian rotation of the control surface).

It is known from basic structural dynamics (Clough and Penizen 1995) that at the undamped natural frequency (ω_i) in the i^{th} elastic mode, inertial and stiffness forces are 180° out of phase and cancel out. Assuming negligible damping, the representation of the forces acting on a system under external loading F , before and at resonance are shown in Fig. 1(a), (b) respectively.

Using above in the first equation of Eq. (3), amplitude of oscillation in the r^{th} elastic mode can be written as

$$e_{or} = \frac{[\omega_r^2 (M_{q\delta})_r - (K_{q\delta})_r] \delta_o}{g_r (K_{qq})_r} \quad (7)$$

Considering lateral dynamics and using Eqs. (1) / (2), (3) and (7), modal amplitude from lateral acceleration response and roll rate response for the r^{th} mode are given by

$$(n_{y_o})_r = \frac{\xi_r [\omega_r^4 (M_{q\delta})_r - \omega_r^2 (K_{q\delta})_r] \delta_o}{g_r (K_{qq})_r} \quad (8)$$

$$(p_o)_r = \frac{\zeta_r [\omega_r^3 (M_{q\delta})_r - \omega_r (K_{q\delta})_r] \delta_o}{g_r (K_{qq})_r} \quad (9)$$

From Eqs. (8) and (9) it is seen that sensor location, natural frequency (aircraft mass, stiffness), inertia coupling and stiffness coupling (control surface mass, stiffness, hinge line offset from center of mass of control surface), modal damping, actuator stiffness and damping are the factors influencing gain amplitude of servoeelastic response. Further, a sensitivity study has been carried out to identify the more critical among these parameters which could be tuned to achieve an accurate analytical estimate of the lateral servoeelastic response.

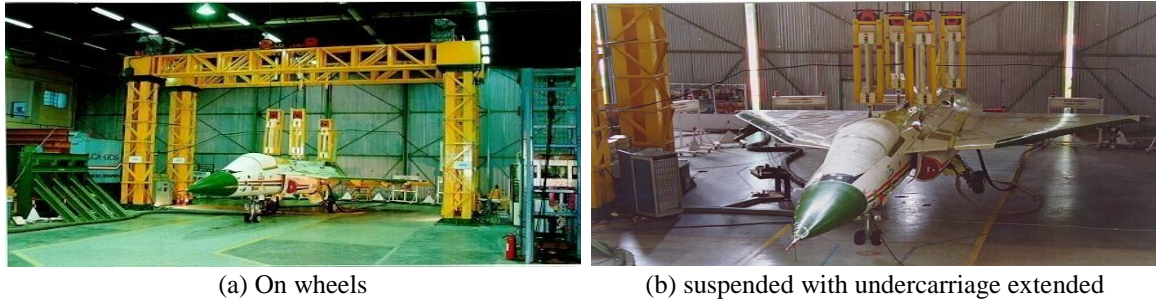


Fig. 2 Aircraft at ground test hangar

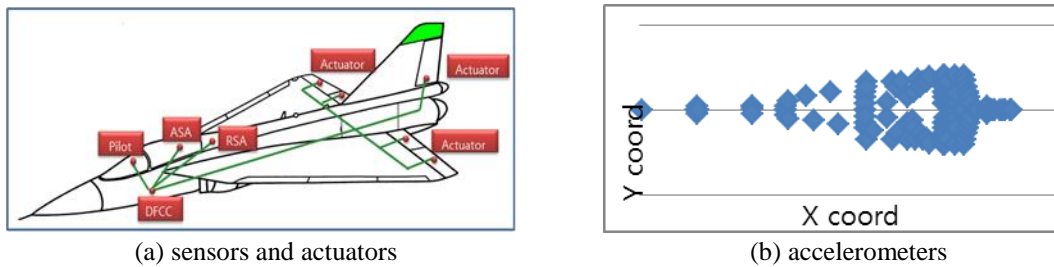


Fig. 3 Aircraft schematic

3. Dynamic tests

Ground vibration tests and structural coupling tests were conducted on a flexible fly-by-wire aircraft. Fig. 2 shows the aircraft at the test hangar). These dynamic tests are mandatory for flight certification. The test data is used for estimating fundamental modes, to determine actual damping values and for validating the finite element (F.E.) models. Since the number of tests are necessarily limited, ideally the analytical and experimental approaches should complement each other. Tests were carried out for various boundary conditions (two cases: aircraft on wheels and suspended with undercarriage extended are shown in Fig. 2(a) and (b) respectively). Test matrix included aircraft configurations with different levels of fuel in internal and external tanks. Various combinations of stores mounted under wing, air-intake and fuselage stations were also tested.

The aircraft has five control surfaces and actuators. The flight control system sensors - accelerometers and rate gyros are mounted on the fuselage as shown in the schematic in Fig. 3(a). For GVT, electrodynamic shakers were mounted at extremities of the aircraft and burst random excitation in required frequency band was input. The advantage of using a burst random excitation is the good signal to noise ratio and avoidance of leakage problems by adopting a uniform or exponential window. Accelerometers were mounted on the aircraft for monitoring structural response during the tests (Fig. 3(b)).

For conducting SCT, the primary control surfaces were excited with stepped sine signals in the desired frequency band. In phase and out of phase excitation of elevons was used to assess longitudinal and lateral responses. Excitation of rudder was used to study directional responses. The input excitation was sent as DC analog signals to control surface actuators which drive the control surface oscillation about hinge lines, thereby generating inertial forces to excite the aircraft.

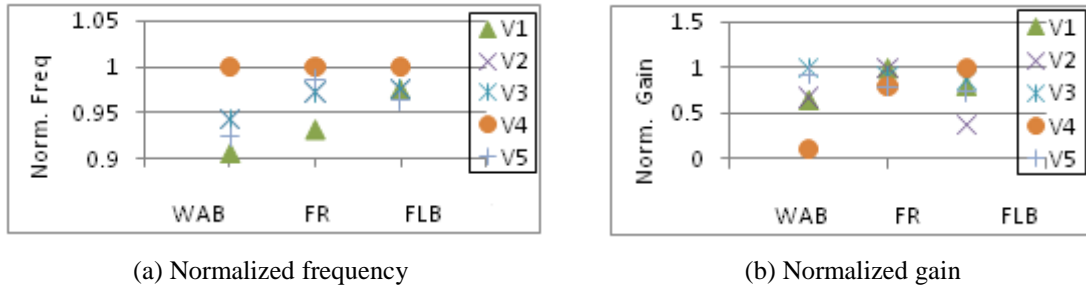


Fig. 4 Scatter in test results of lateral servoelastic response

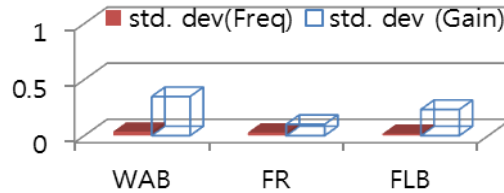


Fig. 5 Standard deviation in test results of lateral servoelastic response: Natural frequencies and gain

Data from five sets of GVT and SCT carried out on the developmental aircraft (versions V1 to V5) have been studied. It was necessary to first validate test results as errors can be introduced due to incorrect fixtures, instrumentation errors (calibration, transducer mounting, overloads), signal processing errors, parameter extraction errors, etc. The scatter in test data with respect to lateral dynamics in terms of natural frequency and gain amplitude of servoelastic responses was computed and is shown for three lateral modes, wing antisymmetric bending (WAB), fuselage roll (FR) and fuselage lateral bending (FLB) in Fig. 4. The standard deviation in the measured natural frequencies across the five aircraft was found to be within 0.1 (Fig. 5). For FR and FLB modes, standard deviation for gain amplitude of response was within 0.2, while for WAB mode it was seen to be around 0.35. The level of scatter in lateral servoelastic responses across aircraft is low, data is consistent and it is assumed that test results are accurate. The validation criterion for servoelastic responses was that the absolute values of normalized test analysis differences should be ≤ 0.03 in respect of natural frequencies and ≤ 0.07 in respect of gain amplitudes.

4. Test analysis correlation

The F.E. model of the aircraft used for estimating servoelastic responses is shown in Fig. 6. The aircraft configuration considered corresponds to full internal fuel with stores present on outboard wing station. The normalized servoelastic response for a unit antisymmetric control surface excitation is studied. For the important modes, wing antisymmetric bending, fuselage roll and fuselage lateral bending, the mode shapes and test-analysis correlation are shown in Figs. 7 to 9. To quantify test-analysis correlation of mode shapes modal assurance criterion (MAC) (Ewins 2000) is computed as

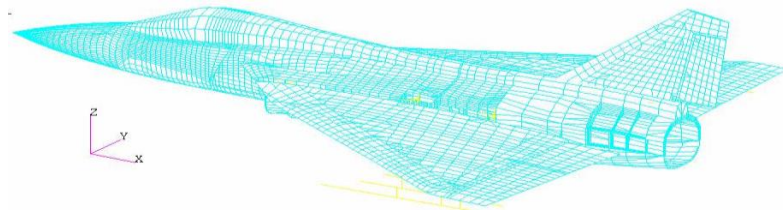
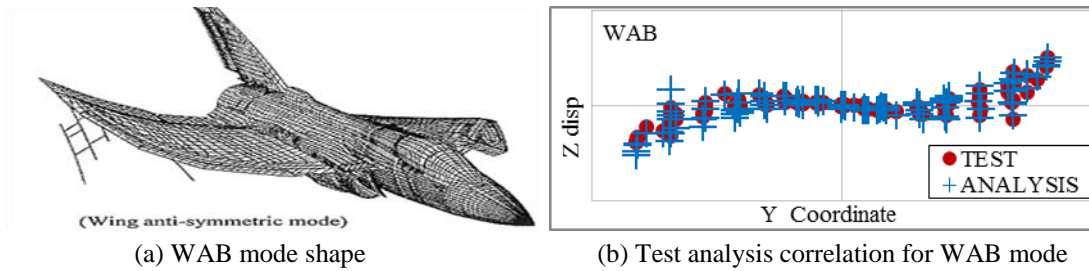


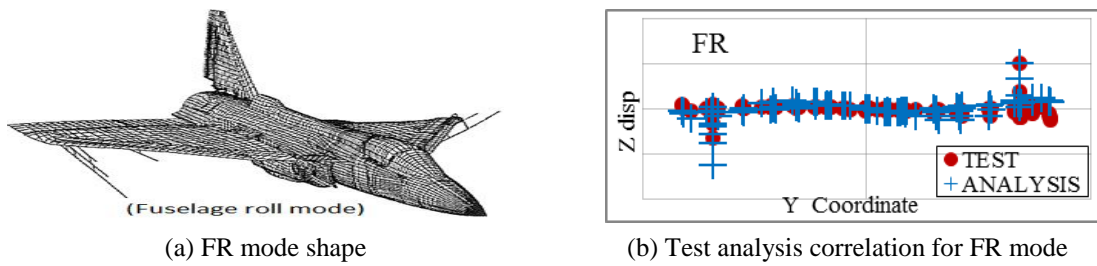
Fig. 6 F.E. model of aircraft under study



(a) WAB mode shape

(b) Test analysis correlation for WAB mode

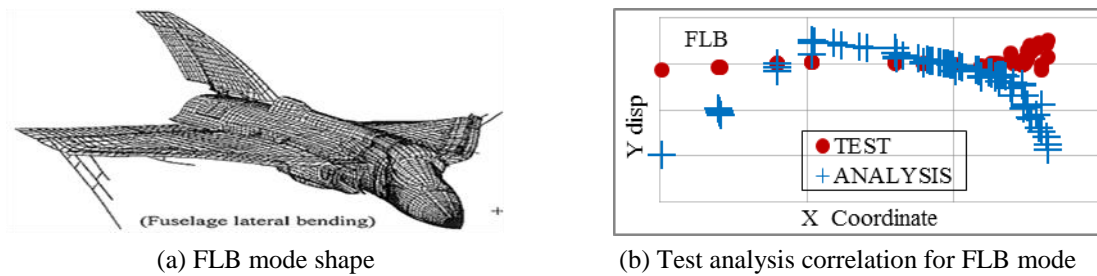
Fig. 7 Wing antisymmetric bending mode



(a) FR mode shape

(b) Test analysis correlation for FR mode

Fig. 8 Fuselage roll mode



(a) FLB mode shape

(b) Test analysis correlation for FLB mode

Fig. 9 Fuselage lateral bending mode

$$MAC_{ij} = \frac{|\{\phi_{Ai}\}^T \{\phi_{Xj}\}|^2}{(\{\phi_{Ai}\}^T \{\phi_{Ai}\})(\{\phi_{Xj}\}^T \{\phi_{Xj}\})} \quad (10)$$

where, ϕ_A and ϕ_X are the analytical and experimental modal vectors respectively. MAC values lie between 0 and 1 and a MAC of 1 indicates an exact correlation. The MAC plot for WAB, FR and

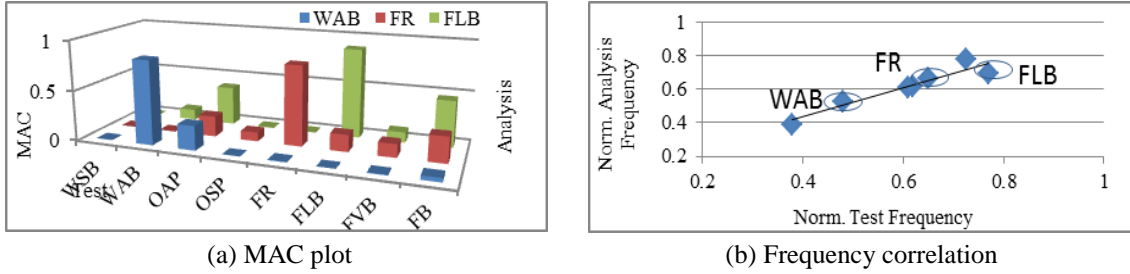


Fig. 10 Test analysis correlation for WAB, FR and FLB

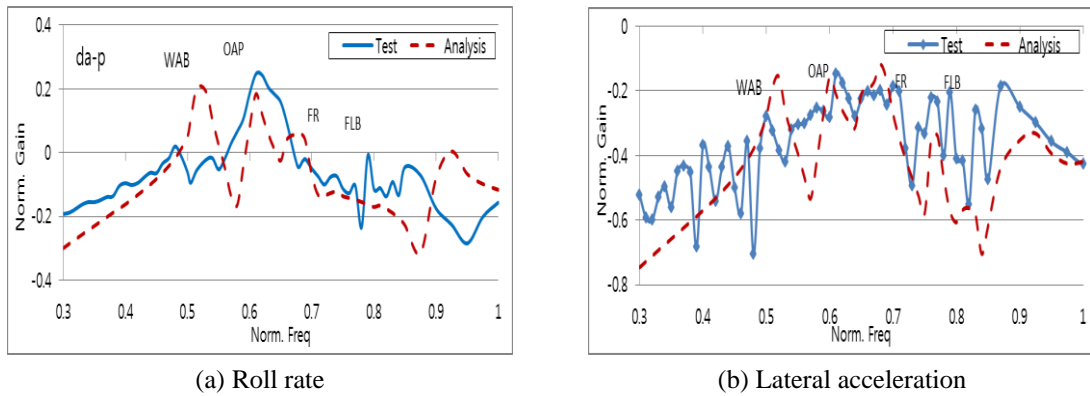


Fig. 11 Test analysis correlation of lateral servoelastic responses

FLB modes with respect to important global aircraft modes estimated from test are shown in Fig. 10(a). The modal vectors for WAB, FR and FLB have an associated MAC value of 0.86, 0.83 and 0.72.

The test-analysis correlation of natural frequencies associated with WAB, FR and FLB modes is shown in Fig. 10(b) and 11. Among the three modes, it is seen that deviation in analytical prediction of natural frequency as compared to experiment is more for FLB, while it is minimum for FR mode.

The initial test analysis correlation for two important lateral response transfer functions, namely roll rate response and lateral acceleration response is shown in Fig. 11. Servoelastic responses are a combination of structural dynamics and control dynamics. The differences in analytical and experimental results can be attributed to local modes of stores which are not captured in analysis due to unmodelled dynamics. Inclusion of non-linear effects like free play in joints and deadband in sensors may improve the response match particularly in the low frequency range. To quantify the degree of correlation, a measure called the enhanced frequency domain assurance criterion (EFDAC) has been used. EFDAC is computed as (Pascual *et al.* 1997)

$$EFDAC(\omega^A, \omega^X) = \frac{\{H(\omega)^A\}^T \{H(\omega)^X\}}{\| \{H(\omega)^A\} \| \| \{H(\omega)^X\} \|} \quad (11)$$

where, $H(\omega)^A$ and $H(\omega)^X$ are the analytical and experimental frequency response functions. EFDAC values lie between -1 and 1 and EFDAC of 1 indicates an exact correlation.

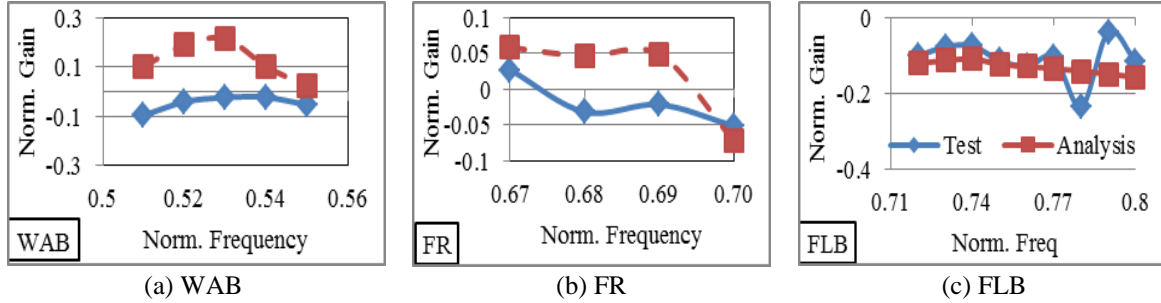


Fig. 12 Test analysis correlation: Frequency windows for three lateral servoelastic modal responses

EFDAC values for windows of frequency chosen for WAB, FR and FLB (Fig. 12) are computed as -0.7, 0.2 and 0.8 respectively. The present study aims to satisfy validation criteria for analysis results established in previous section, namely, normalized frequency deviations within 0.03 and gain amplitude deviations within 0.07 with respect to test results. MAC values for the three modes were ≥ 0.7 and were considered satisfactory.

5. Sensitivity study

5.1 Sensitivity: structural dynamics

The sensitivity of system response y to a system parameter P_i is defined as in Wang, Huang and Zhang (1993)

$$S[y | P_i] = \lim_{\Delta P_i \rightarrow 0} \frac{\Delta y / y}{\Delta P_i / P_i} = \frac{P_i}{y} \frac{\partial y}{\partial P_i} \quad (12)$$

The sensitivity of the natural frequency (ω_r of the r^{th} mode) with respect to P_i is

$$S[\omega_r | P_i] = \frac{P_i}{2\omega_r^2} \{\phi_r\}^T \left(\frac{\partial [K]}{\partial P_i} - \omega_r^2 \frac{\partial [M]}{\partial P_i} \right) \{\phi_r\} \quad (13)$$

where $[M]$, $[K]$ and ϕ_r refer to the mass and stiffness matrices and r^{th} modal vector.

Expressing $\frac{\partial \{\phi_r\}}{\partial P_i}$ as a linear combination of eigen vectors

$$\frac{\partial \{\phi_r\}}{\partial P_i} = \sum_{s=1}^n \alpha_{rs} \{\phi_s\} \quad (14)$$

The sensitivity of the modal vector with respect to P_i is given by

$$S[\phi_{kr} | P_i] = \frac{P_i}{\phi_{kr}} \sum_{s=1}^r \alpha_{rs} \{\phi_s\}, k = 1, 2, \dots, n \quad (15)$$

$$\alpha_{rs} = \begin{cases} \frac{-1}{2} \{\phi_r\}^T \frac{\partial[M]}{\partial P_i} \{\phi_r\}, s = r \\ \frac{1}{\omega_r^2 - \omega_s^2} \{\phi_s\}^T \left(\frac{\partial[K]}{\partial P_i} - \omega_r^2 \frac{\partial[M]}{\partial P_i} \right) \{\phi_r\}, s \neq r \end{cases}$$

However, for a large size problem which is simulated by modeling different types of finite elements, the mass and stiffness matrices are generally nonlinear functions of the parameter P_i . The sensitivities are computed as

$$\frac{\partial M}{\partial P_i} \approx \frac{M(P_i + \Delta P_i) - M(P_i)}{\Delta P_i} \quad (16)$$

$$\frac{\partial K}{\partial P_i} \approx \frac{K(P_i + \Delta P_i) - K(P_i)}{\Delta P_i} \quad (17)$$

5.2 Sensitivity: servoeelastic responses

Differentiation of Eqs. (8), (9) with respect to parameter P_i gives the variation of the modal amplitude of lateral acceleration and roll rate responses with respect to P_i

$$\frac{\partial(K_{qq})_r}{\partial P_i} (n_{y0})_r + (K_{qq})_r \frac{\partial(n_{y0})_r}{\partial P_i} = \frac{\xi_r \delta_0}{g_r} \left[4\omega_r^3 \frac{\partial\omega_r}{\partial P_i} (M_{q\delta})_r + \omega_r^4 \frac{\partial(M_{q\delta})_r}{\partial P_i} - 2\omega_r \frac{\partial\omega_r}{\partial P_i} (K_{q\delta})_r - \omega_r^2 \frac{\partial(K_{q\delta})_r}{\partial P_i} \right] \quad (18)$$

$$\frac{\partial(K_{qq})_r}{\partial P_i} (p_0)_r + (K_{qq})_r \frac{\partial(p_0)_r}{\partial P_i} = \frac{\xi_r \delta_0}{g_r} \left[3\omega_r^2 \frac{\partial\omega_r}{\partial P_i} (M_{q\delta})_r + \omega_r^3 \frac{\partial(M_{q\delta})_r}{\partial P_i} - \frac{\partial\omega_r}{\partial P_i} (K_{q\delta})_r - \omega_r \frac{\partial(K_{q\delta})_r}{\partial P_i} \right] \quad (19)$$

In the modal domain, sensitivity of lateral acceleration and roll rate response for a unit input control surface excitation is simplified as

$$\frac{\partial(n_{y0})_r}{\partial P_i} = \frac{\xi_r}{g_r} \left[2\omega_r \frac{\partial\omega_r}{\partial P_i} (M_{q\delta})_r + \omega_r^2 \frac{\partial(M_{q\delta})_r}{\partial P_i} - \frac{\partial(K_{q\delta})_r}{\partial P_i} \right] \quad (20)$$

$$\frac{\partial(p_0)_r}{\partial P_i} = \frac{\xi_r}{g_r} \left[\frac{\partial\omega_r}{\partial P_i} (M_{q\delta})_r + \omega_r \frac{\partial(M_{q\delta})_r}{\partial P_i} + \omega_r^{-2} \frac{\partial\omega_r}{\partial P_i} (K_{q\delta})_r - \omega_r^{-1} \frac{\partial(K_{q\delta})_r}{\partial P_i} \right] \quad (21)$$

The variations of g and ω , $M_{q\delta}$, $K_{q\delta}$, (functions of mass, stiffness matrices for aircraft and control surface) would be nonlinear with respect to a system parameter P_i (like E , ρ) and are difficult to evaluate. For a large finite element mesh associated with a real life problem, element level changes would be difficult to implement. The extent of the effect of each parameter identified above, namely, sensor location, natural frequency (inertia and stiffness), inertia and stiffness coupling, actuator damping and stiffness on the peak modal responses and their relative significance is therefore studied by a $\pm 10\%$ perturbation of the parameter. Modal damping was varied from 1% to 6%. Above bounds for the parameters were chosen to keep the model updation physically meaningful.

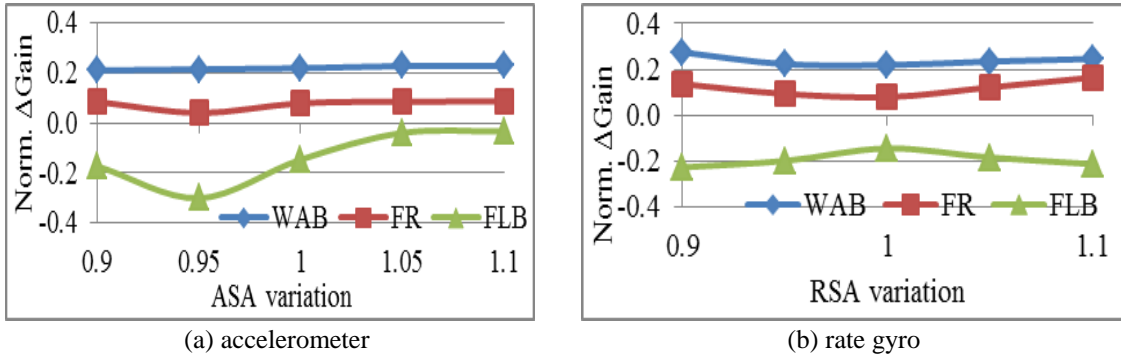


Fig. 13 Test analysis correlation: Effect of sensor location

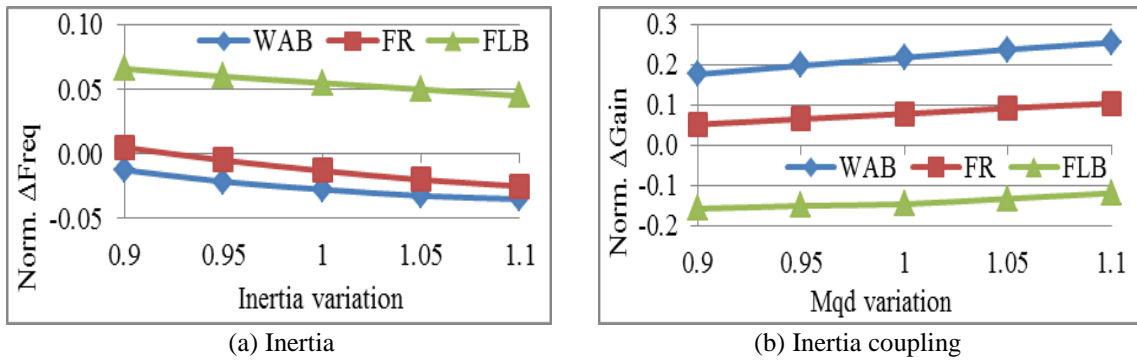


Fig. 14 Test analysis correlation: Effect of perturbation in inertia and inertia coupling

5.3 Effect of sensor location

Based on node point and zero slope point of the fuselage bending mode of the aircraft in baseline configuration, optimal locations were decided for the accelerometer and rate gyro. To study the effect of variation in sensor placement, location of the accelerometer and rate gyro on the fuselage were perturbed by $\pm 10\%$, one at a time. SE responses were computed and differences between test and analytical responses are plotted in Fig. 13(a), (b). It is seen that the present rate gyro placement is optimal and a marginal shift of around 5% in accelerometer location would be beneficial.

5.4 Effect of inertia

The effect of inertia is studied by varying global inertia and inertia coupling terms by $\pm 10\%$. It was seen that gain amplitude is not significantly affected by inertia changes within the above bounds, but as expected there is a change in modal frequency for the three modes considered (Fig. 14(a)). To obtain improved frequency prediction for all three modes from the present model, conflicting requirements exist for values of inertia terms.

The effect of perturbation in inertia coupling terms on aircraft natural frequencies was seen to be negligible. As predicted in Eqs. (8), (9), an increase in inertia coupling terms leads to higher gain amplitude levels (Fig. 14(b)). Similar trends are seen for WAB, FR and FLB modes.

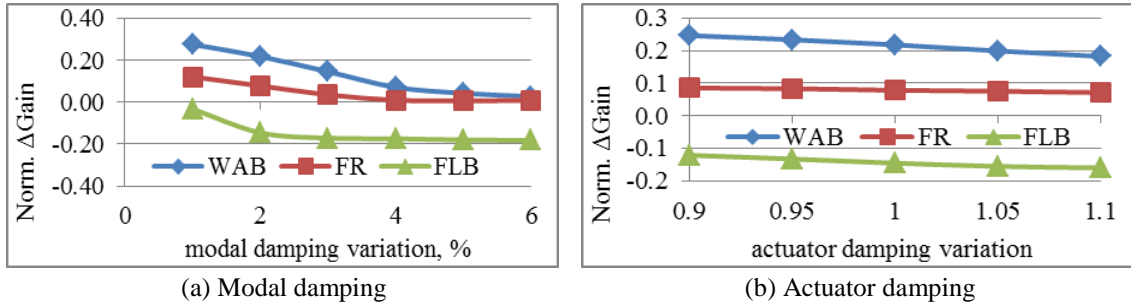


Fig. 15 Test analysis correlation: Effect of perturbation in damping

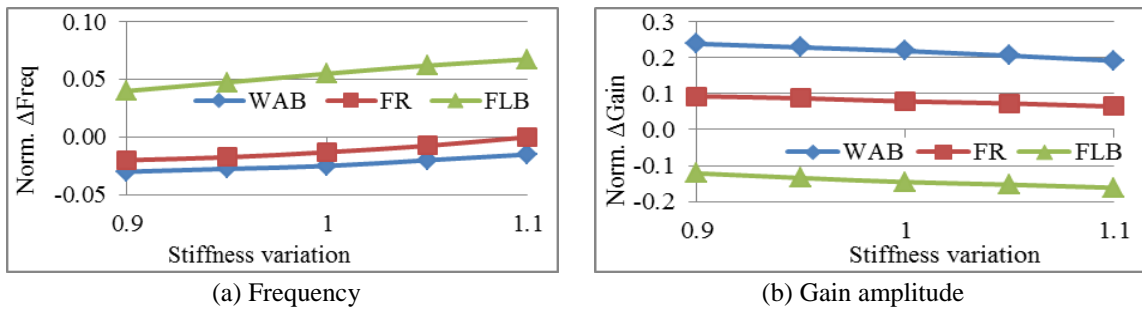


Fig. 16 Test analysis correlation: Effect of perturbation in stiffness

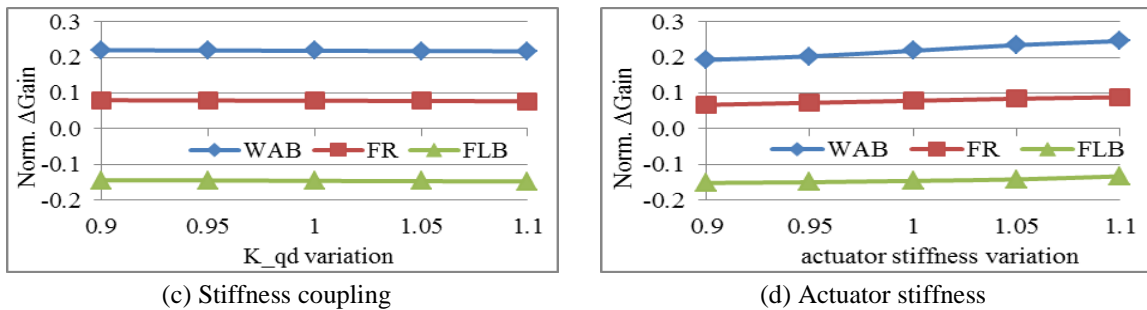


Fig. 16 Test analysis correlation: Effect of perturbation in stiffness coupling/actuator stiffness

5.5 Effect of damping

It is known that damping levels have a significant impact on gain amplitudes of response. The sensitivity to both actuator damping and modal damping was studied separately. Modal damping terms for the flexible modes were perturbed from a value of 1 to 6%. The differences between test results and analytical estimates of lateral servoelastic response due to variation of modal damping is shown in Fig. 15(a). The gain amplitudes show expected inverse relation with modal damping for the range of perturbation considered. Different modes respond differently to changes in damping, change in WAB and FLB being comparable and FR mode being less affected.

The increase in actuator damping values also leads to a reduction in gain amplitude values, with WAB mode being more affected (Fig. 15(b)).

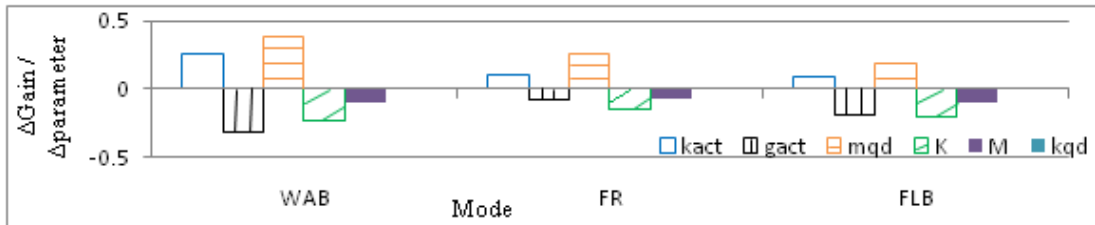


Fig. 17 Extent of effect of each parameter on gain amplitude of the three lateral response modes

5.6 Effect of stiffness

The effect of $\pm 10\%$ perturbation of three different stiffness - modal stiffness, stiffness coupling terms and actuator stiffness on lateral servoelastic response was studied separately. The differences between test values and analytically computed frequencies and gain amplitudes of WAB, FR and FLB due to variation of global stiffness are shown in Fig. 16(a), (b). As expected, natural frequency increases with increase in stiffness. The change in gain amplitudes is higher for the model with decreased modal stiffness. The effect of changes in modal stiffness on the gain amplitude is shown in Fig. 16(b).

It was seen that stiffness coupling terms do not significantly affect gain amplitude of response. The effect on the basic wing and fuselage frequencies is marginal (Fig. 16(c)). However the effect is more significant for higher modes with control surface participation.

The effect of actuator stiffness on natural frequency was seen to be marginal for the three modes. As seen in Fig. 16(d), among the three modes, gain amplitude of response of WAB mode is more sensitive to changes in actuator stiffness.

5.7 Relative influence of critical parameters on servoelastic response

The sensitivity study carried out for a perturbation range of $\pm 10\%$ is used to assess the relative importance of influencing parameters on the three modal SE lateral responses. The variation of the modal gain amplitude for the range of parameter variation ($\Delta(\text{gain}) / \Delta(\text{parameter})$) is computed and plotted in Fig. 17. The range of modal damping variation is different from other parameters and response is not linear for sensor location variation and effects of these two parameters are not shown in Fig. 17. The more effective influencing parameters are modal damping, actuator stiffness, inertia coupling terms, actuator damping, global stiffness and mass. Stiffness coupling terms have negligible influence. Corrections to coupling terms were realized by tuning control surface mass and/or stiffness. The hinge line offset from control surface center of mass was not varied.

6. Multi-parameter study

The problem of model updation in the present study is specific to improving servoelastic response predictions, i.e., frequency and gain amplitude of response for important aircraft global modes. Since lateral dynamics has been considered, modes of interest are WAB, FR and FLB. Of these, WAB mode is more important as it is a lifting surface mode and a fundamental mode and is

capable of being excited easily due to interactions between structural and control dynamics.

For the present aircraft model, FLB frequency and FLB and WAB gain amplitudes are quantities that show more deviation with test results (Figs. 11, 12). It is seen that there is no single common parameter which can be updated within the specified bounds, to achieve a better test-analysis correlation for the three modes in respect of both frequency and gain (Figs. 13-16). For FR mode, initial error in gain amplitude estimation can be adjusted by tuning the assumed modal damping, but a better estimation of FLB frequency and gain would need a combination of parameters. Similarly, for WAB mode, gain amplitude tuning would need adjustment of a combination of parameters. Even in the case where one parameter, for example stiffness, may be tuned for better approximation of lateral aircraft modal frequencies, different values of the parameter need to be adopted for different modes, which is not a feasible option. It is here that additional parameters specific for servoelastic response prediction could play an important role. Multi-parameter updation by considering appropriate combinations of the set of parameters contributing to structure-control coupling is a viable option for obtaining a preliminary updated model. Where required, the model can be further updated by employing more sophisticated or automated methods.

The procedure is illustrated for the aircraft model considered and can be used similarly for servoelastic response updation for any aircraft model. The baseline values (BL) or initial test-analysis deviations in frequency and gain amplitude for WAB, FR and FLB are compared with the effects of varying a single parameter (Table 1). Parameters considered are global stiffness (K), global mass (M), modal damping (g), actuator stiffness (Ak), inertia coupling (Md), actuator damping (Ag) and sensor location (AS / RS). Best values of these parameters (which minimize test-analysis difference of FLB frequency, which shows more deviations with respect to test results) as determined from the sensitivity study are adopted for further response computations. It was seen that updation of the full mass and / or stiffness matrices using above parameteric values results in

Table 1 Test analysis correlation: Effect of single parameter variation on WAB, FR and FLB

1 parameter	WAB		FR		FLB	
	Δ Freq,Hz	Δ Gain,dB	Δ Freq,Hz	Δ Gain,dB	Δ Freq,Hz	Δ Gain,dB
BL	-0.0260	0.2191	-0.0125	0.0789	0.0550	-0.1457
K	-0.0300	0.2357	-0.0200	0.0929	0.0315	-0.1214
M	-0.0350	0.2114	-0.0250	0.0729	0.0450	-0.1543
g	-0.0260	0.0600	-0.0125	0.0357	0.0550	-0.0329
Ak	-0.0260	0.1929	-0.0125	0.0671	0.0550	-0.1514
Md	-0.0260	0.1771	-0.0125	0.0529	0.0550	-0.1571
Ag	-0.0260	0.1829	-0.0125	0.0714	0.0550	-0.1600
RS / AS	-0.0260	0.2191	-0.0125	0.0789	0.0550	-0.1257

Table 2 Test analysis correlation: Effect of seven parameter variation on WAB, FR and FLB

7 parameters	WAB		FR		FLB	
	Δ Freq,Hz	Δ Gain,dB	Δ Freq,Hz	Δ Gain,dB	Δ Freq,Hz	Δ Gain,dB
BL	-0.0260	0.2191	-0.0125	0.0789	0.0550	-0.1457
K,M,g,Md,Ak,Ag,RS/AS	-0.0375	0.0400	-0.0300	0.0257	0.0300	-0.0643

Table 3 Test analysis correlation: Effect of two parameter variation on WAB, FR and FLB

2 parameters	WAB		FR		FLB	
	Δ Freq,Hz	Δ Gain,dB	Δ Freq,Hz	Δ Gain,dB	Δ Freq,Hz	Δ Gain,dB
BL	-0.0260	0.2191	-0.0125	0.0789	0.0550	-0.1457
K,g	-0.0300	0.0800	-0.0200	0.0514	0.0315	-0.0271
M,g	-0.0350	0.0529	-0.0250	0.0314	0.0450	-0.0429
g,Ak	-0.0260	0.0429	-0.0125	0.0286	0.0550	-0.0357
g,Md	-0.0260	0.0371	-0.0125	0.0229	0.0550	-0.0400
Ag,RS/AS	-0.0260	0.1829	-0.0125	0.0714	0.0550	-0.1400

Table 4 Test analysis correlation: Effect of three parameter variation on WAB, FR and FLB

3 parameters	WAB		FR		FLB	
	Δ Freq,Hz	Δ Gain,dB	Δ Freq,Hz	Δ Gain,dB	Δ Freq,Hz	Δ Gain,dB
BL	-0.0260	0.2191	-0.0125	0.0789	0.0550	-0.1457
K,M,g	-0.0375	0.0629	-0.0300	0.0400	0.0300	-0.0300
M,g,Md	-0.0350	0.0343	-0.0250	0.0200	0.0450	-0.0486
K,g,Md	-0.0300	0.0571	-0.0200	0.0371	0.0315	-0.0371
K,g,Ag	-0.0300	0.0714	-0.0200	0.0500	0.0315	-0.0429
M,g,Ak	-0.0350	0.0400	-0.0250	0.0271	0.0450	-0.0500

Table 5 Test analysis correlation: Effect of four parameter variation on WAB, FR and FLB

4 parameters	WAB		FR		FLB	
	Δ Freq,Hz	Δ Gain,dB	Δ Freq,Hz	Δ Gain,dB	Δ Freq,Hz	Δ Gain,dB
BL	-0.0260	0.2191	-0.0125	0.0789	0.0550	-0.1457
K,M,g,Ag	-0.0375	0.0543	-0.0300	0.0386	0.0300	-0.0500
K,M,g,Ak	-0.0375	0.0571	-0.0300	0.0357	0.0300	-0.0357
K,M,g,RS	-0.0375	0.0629	-0.0300	0.0400	0.0300	-0.0257
K,Md,g,Ag	-0.0300	0.0514	-0.0200	0.0343	0.0315	-0.0571
K,g,Ak,Ag	-0.0300	0.0686	-0.0200	0.0457	0.0315	-0.0486
M,g,Md,Ag	-0.0350	0.0300	-0.0250	0.0171	0.0450	-0.0686

improvement of FLB frequency, but has an adverse effect on WAB and FR mode frequencies.

Table 2 shows effect of tuning all seven parameters together, which is seen to be beneficial for gain amplitude updation of all three modes. Possible combinations of two, three, four, five and six parameter values were also studied. Some of the important results are shown in Tables 3 to 7.

Above results show that test-analysis deviations of gain amplitude could be updated for all the three modes to specified tolerances, while prediction of natural frequencies can be further updated. Simultaneous response updation for the three modes can be greatly improved by implementation of parameter changes in appropriate regions or zones. More combinations of parameter values within the specified bounds should also be considered by employing automated methods. Updated SE responses are shown for one case, i.e., by updating the five parameter combination of *K, g, Md,*

Table 6 Test analysis correlation: Effect of five parameter variation on WAB, FR and FLB

5 parameters	WAB		FR		FLB	
	Δ Freq,Hz	Δ Gain,dB	Δ Freq,Hz	Δ Gain,dB	Δ Freq,Hz	Δ Gain,dB
BL	-0.0260	0.2191	-0.0125	0.0789	0.0550	-0.1457
K,M,g,Ak,Ag	-0.0375	0.0500	-0.0300	0.0343	0.0300	-0.0600
K,M,g,Md,Ag	-0.0375	0.0457	-0.0300	0.0314	0.0300	-0.0643
M,g,Md,Ag,Ak	-0.0350	0.0243	-0.0250	0.0114	0.0450	-0.0743
K,g,Md,Ag,Ak	-0.0300	0.0443	-0.0200	0.0286	0.0315	-0.0614
K,M,g,Md,Ak	-0.0375	0.0429	-0.0300	0.0300	0.0300	-0.0571

Table 7 Test analysis correlation: Effect of six parameter variation on WAB, FR and FLB

6 parameters	WAB		FR		FLB	
	Δ Freq,Hz	Δ Gain,dB	Δ Freq,Hz	Δ Gain,dB	Δ Freq,Hz	Δ Gain,dB
BL	-0.0260	0.2191	-0.0125	0.0789	0.0550	-0.1457
K,M,g,Md,Ag,Ak	-0.0375	0.0400	-0.0300	0.0257	0.0300	-0.0743
K,M,g,Md,Ag,RS	-0.0375	0.0457	-0.0300	0.0314	0.0300	-0.0571
K,Md,g,Ak,Ag,RS	-0.0300	0.0443	-0.0200	0.0286	0.0315	-0.0557

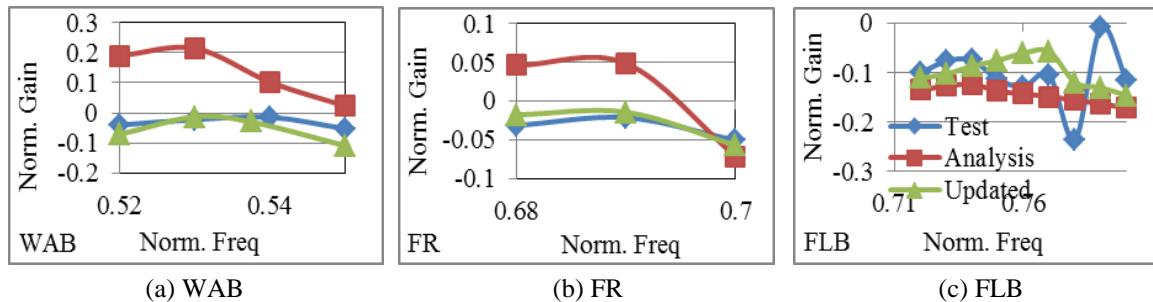


Fig. 18 Test analysis correlation: Updated lateral SE response

Ak and Ag (Fig. 18). It is seen that gain amplitudes for all three modal responses are improved and FLB frequency may be slightly updated, as per requirements. EFDAC values computed for updated responses of WAB, FR and FLB are 0.9, 0.95 and 0.84 respectively.

9. Conclusions

Important parameters influencing lateral servoelastic response of a generic flexible airvehicle have been identified. A sensitivity study has indicated the extent of influence of each parameter. Based on this, a multi-parameter model updation approach has been implemented to realize improved test analysis correlation of servoelastic responses. The method is generic and can be applied to any flexible aircraft model.

In the present study, the multi-parameter updation approach is illustrated on a flexible aircraft model with test data generated from structural coupling tests. Different modal responses from

lateral dynamic transfer functions were updated simultaneously in terms of both gain and frequency. The prediction of gain amplitude of response could be updated within specified tolerances resulting in an improved analytical model. Simultaneous updation of frequency and gain amplitude can be achieved by identification and application of corrections to appropriate zones in the model. More combinations of values of the influencing parameters within specified bounds also can be studied through automated methods. Servoelastic response prediction using the updated analytical model was found to be beneficial for an initial assessment of the effects of mounting different store combinations or for predicting effects of minor changes in the airframe structure.

Acknowledgments

The first author thanks the Technology Director (AirFrame) and Program Group Director (ADA) and Director (CA) for their permission to publish this paper.

References

- Allen, M.G., Reardon, M.G. and Gordon, F.W. (1986), "Use of the flight simulator in performing AFTI/F-16 airplane aeroservoelastic analysis", *In 27th Structures, Proceedings of the Structural Dynamics and Materials Conference*.
- Arnold, J.I. and Murphy, F.B. (1976), "B-52 control configured vehicles: Flight test results", N76-31139, The Boeing Company, Wichita Division, 75-89.
- Bart, P., Héctor, C., Raul, D., Jesús, A., Ahlquist, J.R., Carreño, J.M., Wim, H., Alain, R., Gonzalo, G., Jeroen, D. and Jan, D. (2008), "Modern solution for ground vibration testing of large aircraft", *IMAC 26*, Orlando, U.S.A.
- Becker, J. and Vacarro, V. (1995), "Ground structural coupling testing and model updating in the aeroservoelastic qualification of a combat aircraft", *80th Meeting of the AGARD SMP*, Rotterdam.
- Becker, J. Caldwell, B. and Vaccaro, V. (2000), "The interaction of flight control system and aircraft structure", Daimler Chrysler Aerospace Munich Military Aircraft, Germany.
- Clough, R.W. and Penzien, J. (1995), *Dynamics of Structures*, 3rd Edition, Computers and Structures Inc., California, U.S.A.
- Ewins, D.J. (2000), "Model validation: Correlation for updating", *Sadhana*, **25**(3), 221-234.
- Felt, L.R., Hutsell, L.J., Noll, T.E. and Cooley, D.E. (1979), "Aeroservoelastic encounters", *J. Aircraft*, **16**(7), 477-483.
- Joshi, A., Srinivasan, P., Narayanaswamy, I. and Hemalatha, E. (2014), "Identification of critical parameters for improved servoelastic response predictions of a flexible aircraft", *National Seminar on Aerospace Structures (18th NASAS)*, Nagpur, India, December.
- Lai, C. and Yang, C. (1994), "Structural coupling ground test for structural filter design on aircraft", *Proceedings of the 36th Conference on Aeronautics and Astronautics*, R.O.C., Taiwan, December.
- Luber, W. (2009), "Aeroservoelastic design and verification of a combat aircraft", *Proceedings of the IMAC-XXVII*, Orlando, Florida, U.S.A., February.
- Mottershead, J.E. and Friswell, M.I. (1993), "Model updating in structural dynamics: A Survey", *J. Sound Vib.*, **167**(2), 347-375.
- Noll, T.E. (1990), "Aeroservoelasticity", NASA TM 102620, March.
- Pascual, R., Golinval, J.C. and Razeto, M. (1997), "A frequency domain correlation technique for model correlation and updating", *IMAC XV*.
- Peloubet, R.P. (2006), "Flutter prevention handbook: A preliminary collection, Part D: Aeroservoelastic

- Instability”, Case Study A, NASA/TP-2006-212490, 2(2).
- Pickerel, C.R., Foss, G.C., Phillips, A., Allemang, R.J. and Brown, D.L. (2006), “New concepts in aircraft ground vibration testing”, *Sound Vib.*, **40**(10), 12-17.
- Voraceck, D.F. and Clarke, R. (1991), “Buffet induced structural/flight control system interaction of the X-29A aircraft”, NASA Ames Research Center, NASA TM-101735, California.
- Wang, J., Zhi-Chu Huang, Z. and Zhang, Q. (1993), “Sensitivities of mechanical structures to structural parameters”, *Comput. Struct.*, **49**(3), 557-560.
- Wray, W.R. (1999), “F-22 structural coupling lessons learned, lockheed martin tactical aircraft systems”, Presented at the RTO AV Specialists Meeting on “Structural aspects of flexible aircraft control”, Canada, October.